Aerospace Science and Technology 76 (2018) 386–393

Contents lists available at ScienceDirect

Aerospace Science and Technology

www.elsevier.com/locate/aescte

Attitude stabilization of flapping micro-air vehicles via an observer-based sliding mode control method

Xuan-Toa Tran [a], Hyondong Oh [a,*], In-Rae Kim [b], Seungkeun Kim [b]

[a] School of Mechanical and Nuclear Engineering, Ulsan National Institute of Science and Technology, Ulsan 44919, South Korea
[b] Department of Aerospace Engineering, Chungnam National University, 99 Daehak-ro, Yuseong-gu, Daejeon 305-764, South Korea

ARTICLE INFO

Article history:
Received 20 September 2017
Received in revised form 5 December 2017
Accepted 10 January 2018
Available online 20 February 2018

Keywords:
Flapping micro-air vehicles
Attitude stabilization
Finite-time observer
Sliding mode control

ABSTRACT

This paper introduces an observer-based sliding mode control strategy for stabilizing the attitude of flapping micro-air vehicles in the presence of unknown uncertainties and external disturbances. First, a finite-time observer is designed to estimate the lumped disturbances. Next, a controller is developed to provide attitude stabilization with high robustness where the lumped disturbances could be completely rejected after a finite amount of time. The stability of the closed-loop system is rigorously proven. By employing MATLAB/Simulink software, a numerical simulation example including a comparison between the proposed method and a conventional sliding mode controller is provided to illustrate the effectiveness of the proposed method and to confirm the theoretical results.

1. Introduction

In the last two decades, the research topic of insect-mimicking flapping micro-air vehicles (MAVs) has attracted much attention because of its potential benefits for both civil and military applications such as inspections in hazardous working conditions, search and rescue, surveillance and tracking and reconnaissance [1]. An ability of sustained hovering flight as well as great maneuverability of insect/birds are of great interest, which motivated researchers to develop flapping MAVs possessing similar flight mechanisms. In [1] and [2], comprehensive surveys of the recent advances in wing kinematics, aerodynamics and dynamics model, stability analysis and flight control design developments of flapping MAVs are presented. In recent years, most of researchers have focused on several aspects to improve the performance in the analysis, modeling, and design of flapping MAVs. Zhang and Rossi [3] have provided a comprehensive survey of designing proper mechanisms for flapping transmission. Nan et al. [4] has described a method of optimized wing design for a hummingbird-like MAV, which leads to increase the wing lift forces. In [5], an onboard/offboard sensor fusion has been developed to obtain free-flight data that are very important in the analysis and modeling of flapping flight. The study in [6] has presented a computationally efficient approach to achieve trim solutions by combining a computational fluid dynamics (CFD) with a flight dynamics model. As indicated in [1,2] and the analysis in the recent works [3–6], the created flapping MAVs have complex structures, highly nonlinear kinematics and dynamics and inherent instability. The flight control design mission, therefore, has become a key research challenge evidenced by the relatively limited number of relevant papers in the literature. For instance, control problems of flapping MAVs are carried out by using PID control [7–9] or optimal control techniques such as Linear Quadratic Regulator/Linear Quadratic Gaussian [10] and pole placement [11].

Although the above-mentioned methods have been successfully applied to control flapping MAVs in simulations or experiments, they are quite limited in terms of real-time applications. The reason is that those methods are developed based on standard linear models, which requires the exact knowledge of nonlinear dynamics; those methods only work well in a small region about an operating point. In addition, possible uncertainties and external disturbances have not been investigated completely. In recent years, few remarkable results [12–14] have been introduced to address the control problem of flapping MAVs concerning such uncertainty and disturbances. The methods in [12,13] have been established based upon the sliding mode control (SMC) technique that has been widely ulitized in many engineering problems thanks to its distinguished properties such as simple design procedure and robustness in the presence of uncertainties and disturbances [15]. Designing the conventional SMC consists of two main steps (see [15,16]): First, defining a sliding mode surface with desired sliding mode dynamics; next, establishing a discontinuous control signal to guarantee the finite-time convergence of the system states to the desired sliding surface. Bluman et al. [12] has applied both

* Corresponding author.
E-mail address: h.oh@unist.ac.kr (H. Oh).

https://doi.org/10.1016/j.ast.2018.01.045
1270-9638/

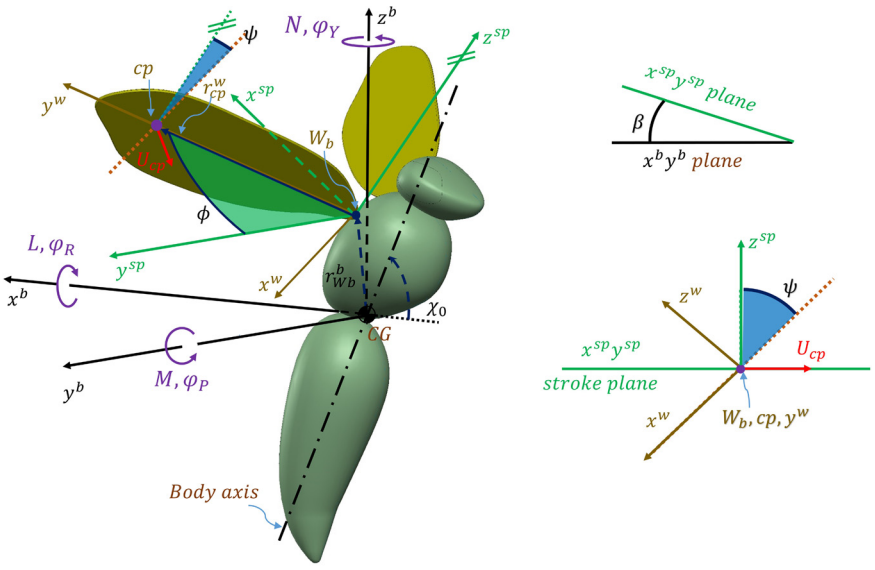

Fig. 1. A schematic model of flapping MAVs. (For interpretation of the colors in the figure(s), the reader is referred to the web version of this article.)

the conventional SMC and second-order SMC to flapping MAVs restricted to the pitch plane assuming that the upper bound of the uncertainties and disturbances are known. This assumption might pose difficulties in flight control design, especially for flapping MAVs systems. Additionally, the control laws in the equations (13) and (17) of the paper [12] may lead to the well-known chattering phenomenon, a main drawback of SMC design. Chirarattannanon et al. [13] has proposed a control strategy based on SMC techniques and adaptive control to improve closed-loop system performance in the presence of uncertain parameters generated by manufacturing imperfections and lack of full knowledge of the system. Although, their work was confirmed by successful experimental results, the adaptive laws (14) and (24) in [13] may make the gains overestimated against uncertainties as a common problem mentioned in [17]. In [14], a similar overestimation of gains might also happen and only the constant or slowly time-varying disturbances has been considered, even though the interesting results has been presented. In order to remove the effects of uncertainties and external disturbances, disturbance-observer based control is a good solution along with adaptive control techniques [18–20]. A thorough search of the relevant literature indicates that observer-based control is rarely employed for control design of flapping MAVs even through they are commonly applied to other engineering systems.

Motivated by the discussion above, this work aims to establish an ob-server-based sliding mode control strategy to obtain the attitude stabilization of flapping MAVs in spite of unknown uncertainties and external disturbances. The employed linear model of flapping MAVs is based on the unit-quaternion concept and Cheng's work [8]. The stability of the controlled flapping MAVs system is proven using Lyapunov stability theory and finite-time control theory.

The remainder of the paper is organized as follows. Section 2 provides the description of considered flapping MAVs. Dynamics of flapping MAVs and its linear model used in control design procedure are presented in Section 3. Section 4 describes the design of the proposed control approach as well as stability analysis. Numerical simulation results and discussion are given in Section 5 to show the efficiency of the suggested control method. The conclusions are drawn in Section 6.

2. Flapping MAVs model

The section describes the flapping micro-air vehicle (MAV) model considered in this article. Fig. 1 depicts a schematic model of the flapping MAVs including the coordinate frames and wing kinematics parameters. Let $CG - x^b y^b z^b$, $Wb - x^{sp} y^{sp} z^{sp}$ and $Wb - x^w y^w z^w$ be body-fixed frame, stroke-plane frame and wing frame, respectively. The origin of the body-fixed frame is the position of the center of gravity (CG) of the whole MAVs, and the origin of the stroke frame and wing frame are located at the wing base (Wb). $x^b z^b$ plane coincides with the symmetric plane of the flapping MAV body containing the body axis; and, in hovering flight, x^b axis is horizontal and points backward and z^b is vertical and points upward. The so-called stroke-plane angle β is the angle of $x^{sp} y^{sp}$ plane and $x^b y^b$ plane, and y^b and y^{sp} have the same direction. The orange dashed line in Fig. 1 is along with wing chord; $\chi_0, cp, U_{cp}, r^w_{cp}$ and r^b_{Wb} stand for free body angle with respect to the horizontal plane, center of wing pressure, velocity of cp, the position of cp with respect to the wing frame (cp is also in $x^{sp} y^{sp}$ plane), and the position of Wb with respect to the body-fixed frame, respectively.

The kinematics of flapping MAVs, via the coordinate systems above, represents wing and body motion. The body kinematics can be described by the free body angle χ_0 and the stroke-plane angle β, while the wing kinematics considered in this article can be represented by a stroke angle ϕ, the wing sweeps about z^{sp} axis in the wing-fixed frame, and a rotation angle ψ the wing rotates about y^w. This hovering mode is called the water-treading mode that discussed in details in [21,22]. Therefore, the wing kinematics could be modeled with two degree-of-freedom (2-DOF), which is the same as that described by Cheng and Deng [8], including the stroke angle $\phi(t) = (\Phi/2)\sin(2\pi f t)$ and the rotation angle $\psi(t) = (\Psi/2)\cos(2\pi f t)$. Here Φ is stroke angle magnitude, Ψ represents maximum rotation angle and f is flapping frequency. The angle of attack $\alpha(t)$ is determined by $\alpha(t) = \pi/2 - \psi(t)$.

The wing and body movement result in aerodynamic forces that are formed based on the quasi-steady state model [23], in which the force expressions developed for two-dimensional thin aerofoils translating under the conditions such as constant velocity and constant angle of attack can be utilized for time-varying three-dimensional flapping wings [24]. As a result, the total normal and tangential aerodynamic forces completely derived in [24] could be given by

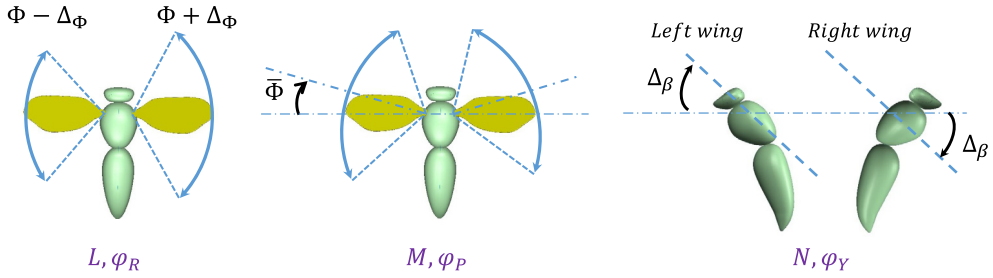

Fig. 2. Control variables (refer to [8]).

$$F_N(t) = \frac{1}{2}\rho A_w U_{cp}\left[C_N(\alpha) U_{cp} + C_{\text{rot}}\hat{c}c_m\dot{\alpha}\right] \quad (1)$$

$$F_T(t) = \frac{1}{2}\rho A_w C_T(\alpha) U_{cp}^2 \quad (2)$$

where ρ is the density of air, A_w is the wing area, c_m is maximum wing chord length, $\hat{c}$ is the normalized rotational chord, and $C_N(\alpha)$, C_{rot}, and $C_T(\alpha)$ are force coefficients expressed by

$$C_N(\alpha) = 3.4\sin\alpha$$

$$C_T(\alpha) = \begin{cases} 0.4\cos^2(2\alpha), & 0 \le \alpha \le 45^o \\ 0, & \text{otherwise} \end{cases}$$

$$C_{rot} = 2\pi\left(\frac{3}{4} - \hat{x}_0\right)$$

where $\hat{x}_0$ usually equals to 1/4 for general flying insects. The generated forces and torques in the body frame cause the motion of the flapping MAV.

3. Dynamics of flapping MAVs and model for control design

3.1. Dynamics of flapping MAVs

In this study, it is assumed that the gravitational acceleration (g) is constant, and the flapping MAV is a 6-DOF rigid body with mass m, moments of inertia about body-fixed axes (I_{xx}, I_{yy}, I_{zz}), and non-zero cross-product of inertia I_{xz}. Under aerodynamics moments $\tau = [L, M, N]^T$, the attitude dynamics and kinematic of motions, that are taken from [24,25], consist of a set of differential equations regarding angular velocity ($\omega = [\omega_1, \omega_2, \omega_3]^T$) and Euler angles Roll–Pitch–Yaw $\varphi = (\varphi_R, \varphi_P, \varphi_Y)$ given by the following moment equations

$$I_b\dot{w} + \omega \times I_b\omega = \tau + \tau_d \quad (3)$$

where τ_d is external disturbance torques and

$$I_b = \begin{bmatrix} I_{xx} & 0 & -I_{xz} \\ 0 & I_{yy} & 0 \\ -I_{xz} & 0 & I_{zz} \end{bmatrix},$$

and kinematic equations

$$\begin{bmatrix} \dot{\varphi}_R \\ \dot{\varphi}_P \\ \dot{\varphi}_Y \end{bmatrix} = \begin{bmatrix} 1 & \sin\varphi_R\tan\varphi_P & \cos\varphi_R\tan\varphi_P \\ 0 & \cos\varphi_R & -\sin\varphi_R \\ 0 & \sin\varphi_R\sec\varphi_P & \cos\varphi_R\sec\varphi_P \end{bmatrix} \begin{bmatrix} \omega_1 \\ \omega_2 \\ \omega_3 \end{bmatrix} \quad (4)$$

For the attitude control design purpose, we use the unit-quaternion concept [26] to describe the attitude kinematics of flapping MAVs as follows

$$\begin{cases} \dot{q} = \frac{1}{2}T(Q)\omega \\ \dot{q}_4 = -\frac{1}{2}q^T\omega \end{cases} \quad (5)$$

where $Q = [q^T, q_4]^T$ is the unit quaternion including the vector part $q = [q_1, q_2, q_3]^T$ and the scalar part q_4, and

$$T(Q) = \begin{bmatrix} q_4 & -q_3 & q_2 \\ q_3 & q_4 & -q_1 \\ -q_2 & q_1 & q_4 \end{bmatrix}.$$

3.2. Model for control design

Now, a model that will be employed in the control design procedure is given. The flight of a flapping MAV is carried out in a hovering flight condition, and suppose that the flight dynamics is restricted to 3-DOF angular motions. Based on the small perturbation theory, Cheng and Deng [8] have established a linear approximation model of the near-hover attitude dynamics. In this article, we introduce an attitude dynamics model modified from equation (6) in [8], as

$$\begin{cases} \dot{q} = \frac{1}{2}T(Q)\omega \\ \dot{\omega} = A\omega + Bu + d(t) \end{cases} \quad (6)$$

with A and B are taken from [8]

$$A = \begin{bmatrix} C_4L_p & 0 & C_1N_r \\ 0 & C_3M_q & 0 \\ C_1L_p & 0 & C_2N_r \end{bmatrix}, B = \begin{bmatrix} C_4L_{\Delta\Phi} & C_1N_{\Delta\beta} & 0 \\ 0 & 0 & C_3M_{\bar{\Phi}} \\ C_1L_{\Delta\Phi} & C_2N_{\Delta\beta} & 0 \end{bmatrix}$$

where C_1, C_2, C_3 and C_4 are defined by

$$C_1 = \frac{I_{xz}}{I_{xx}I_{zz} - I_{xz}^2}, C_2 = \frac{I_{xx}}{I_{xx}I_{zz} - I_{xz}^2}$$

$$C_3 = \frac{1}{I_{yy}}, C_4 = \frac{I_{zz}}{I_{xx}I_{zz} - I_{xz}^2},$$

and the estimations of stability derivatives (L_p, M_q, N_r) and control derivatives $(L_{\Delta\Phi}, M_{\bar{\Phi}}, N_{\Delta\beta})$ are obtained based on the models of flapping counter-torque and flapping counter-force (see [8,27] for the detailed description of these derivatives). It is assumed that control matrix B is full rank [28]. The control input $u = [\Delta\Phi, \bar{\Phi}, \Delta\beta]^T$ is chosen to be the same as that in [8], and as illustrated in Fig. 2, roll torque L, pitch torque M, and yaw torque N are controlled through appropriate change of $\Delta\Phi, \bar{\Phi}$, and $\Delta\beta$ respectively. Besides, unknown lumped disturbance vector $d(t) = [d_1(t), d_2(t), d_3(t)]^T$ includes modeling uncertainties and external disturbances.

The aim of the article is to introduce an observer-based control method to achieve asymptotic attitude stabilization of the flapping MAV in the presence of unknown lumped disturbances. The proposed control strategy is presented in the next section.

4. Control strategy design

4.1. Finite-time observer design

For simplified expression through this article, we will use the following notation

$$\lfloor\sigma\rceil^{\upsilon} = \begin{bmatrix} |\sigma_1|^{\upsilon}\text{sign}(\sigma_1) \\ |\sigma_2|^{\upsilon}\text{sign}(\sigma_2) \\ \cdots \\ |\sigma_n|^{\upsilon}\text{sign}(\sigma_n) \end{bmatrix}$$

and $\lfloor\sigma\rceil^0 = \text{sign}(\sigma)$ where $\sigma = [\sigma_1, \sigma_2, \ldots, \sigma_n]^T$,

$L^{[\upsilon]} = \text{diag}\left(L_1^{\upsilon}, L_2^{\upsilon}, L_3^{\upsilon}\right)$ where $L = [L_1, L_2, L_3]^T$.

Inspired by [29] and [30], for the system (6), we introduce an observer that estimates unknown lumped disturbances $d(t)$ having the following structure

$$\begin{aligned} \dot{z}_0 &= -\lambda_n L^{\left[\frac{1}{n+1}\right]}\lfloor z_0 - \omega\rceil^{\frac{n}{n+1}} + A\omega + Bu + z_1 \\ \dot{z}_k &= -\lambda_{n-k} L^{\left[\frac{k+1}{n+1}\right]}\lfloor z_0 - \omega\rceil^{\frac{n-k}{n+1}} + z_{k+1} \\ \dot{z}_n &= -\lambda_0 L^{[0]}\lfloor z_0 - \omega\rceil^0 \\ \hat{\omega} &= z_0, \hat{d}^{(k-1)} = z_k, \hat{d}^{(n-1)} = z_n, \end{aligned} \tag{7}$$

where the coefficients $\lambda_0, \lambda_k, (k = 1, \ldots, n-1)$ and λ_n are positive constants; $\hat{\omega}, \hat{d}^{(k-1)}$ and $\hat{d}^{(n-1)}$ are the estimates of $\omega, d^{(k-1)}(t)$ and $d^{(n-1)}(t)$, respectively. In addition, $L = [L_1, L_2, L_3]^T$ with $L_i > 0$ is a Lipschitz constant of the $(n-1)$th derivative of $d_i(t), (i = 1, 2, 3)$.

Combining (6) and (7), and defining errors $e_0 = \hat{\omega} - \omega, e_k = \hat{d}^{(k-1)} - d^{(k-1)}(t)$ and $e_n = \hat{d}^{(n-1)} - d^{(n-1)}(t)$, we get

$$\begin{aligned} \dot{e}_0 &= -\lambda_n L^{\left[\frac{1}{n+1}\right]}\lfloor e_0\rceil^{\frac{n}{n+1}} + e_1 \\ \dot{e}_k &= -\lambda_{n-k} L^{\left[\frac{k+1}{n+1}\right]}\lfloor e_0\rceil^{\frac{n-k}{n+1}} + e_{k+1} \\ \dot{e}_n &\in -\lambda_0 L^{[0]}\lfloor e_0\rceil^0 + [-L, L]. \end{aligned} \tag{8}$$

Therefore, according to [30], by selecting proper coefficients, the finite-time stability of (6) is guaranteed, which implies that $e_0 = 0, e_k = 0$ and $e_n = 0$ could be obtained in finite time.

Remark 1. Obviously, there exist positive constants ϵ_k $(k = 1, 2, \ldots, n-1)$ satisfying $||e_k|| \le \epsilon_k, \forall t \ge 0$.

4.2. Observer-based control law design

Before presenting the main results, some necessary lemmas employed in the control law design are provided as follows.

Lemma 1. [31] *A direct result of Jensen's inequality is given by*

$$\left(\sum_{i=1}^{3}\theta_i^{\upsilon_2}\right)^{1/\upsilon_2} \le \left(\sum_{i=1}^{3}\theta_i^{\upsilon_1}\right)^{1/\upsilon_1}, 0 < \upsilon_1 < \upsilon_2, \theta_i \ge 0. \tag{9}$$

Lemma 2. [32] *Suppose that a continuous, positive definite function $V(x)$ exists so that*

$$\dot{V}(x) + c_1 V(x) + c_2 V^{\nu}(x) \le 0 \tag{10}$$

where $c_1 > 0, c_2 > 0$ and $0 < \nu < 1$. Then, for any initial condition $x_0 = x(t_0)$, $V(x)$ converges to zero in a finite time t_1 satisfying

$$t_1 \le t_0 + \frac{1}{c_1(1-\nu)}\ln\frac{c_1 V^{1-\nu}(x_0) + c_2}{c_2} \tag{11}$$

The first step of the design procedure is to establish a sliding mode surface that possesses a desired dynamics whenever the sliding motion happens. For the system (4), a sliding mode surface is defined as

$$s = \omega + \Gamma q \tag{12}$$

where $s = [s_1, s_2, s_3]^T$ and $\Gamma = \text{diag}(\gamma_1, \gamma_2, \gamma_3)$ with $\gamma_i > 0$ $(i = 1, 2, 3)$.

Remark 2. The form of sliding surface (12) is similar to that in the results of the paper [33]. It is easy to show that after the system trajectories reach the sliding surface, i.e., $s = 0$, the asymptotic attitude stabilization could be obtained, i.e., $\lim_{t\to\infty} q = 0$.

Next, the main result of the article is summarized by the following theorem.

Theorem 1. *Consider the system described by (6) with the sliding mode surface defined as (12). If the control law is designed as*

$$u = -B^{-1}\left[\left(A + \frac{1}{2}\Gamma T(Q)\right)\omega + \hat{d} + \kappa_1 s + \kappa_2\lfloor s\rceil^{\nu}\right] \tag{13}$$

where $\kappa_1 > 1/2, \kappa_2 > 0$ and $0 < \nu < 1$, then the sliding motion is established in finite time, i.e., $s = 0, \forall t \ge t_r$, here $t_r > 0$ is reaching time, and the asymptotic attitude stabilization of flapping MAVs, in turn, is achieved.

Proof. Taking the time derivative of the sliding surface (12) along the trajectories of (6), one obtains

$$\begin{aligned} \dot{s} &= \dot{\omega} + \Gamma\dot{q} \\ &= A\omega + Bu + d(t) + \frac{1}{2}\Gamma T(Q)\omega. \end{aligned} \tag{14}$$

Substituting (13) into (14) and using (8), we have

$$\begin{aligned} \dot{s} &= -\kappa_1 s - \kappa_2\lfloor s\rceil^{\nu} + d(t) - \hat{d} \\ &= -\kappa_1 s - \kappa_2\lfloor s\rceil^{\nu} - e_1. \end{aligned} \tag{15}$$

Now, we consider a positive definite function as

$$V = \frac{1}{2}s^T s. \tag{16}$$

Combining its derivative with (15) leads to

$$\dot{V} = -\kappa_1 s^T s - \kappa_2 s^T\lfloor s\rceil^{\nu} - s^T e_1. \tag{17}$$

First, we will show that all signals of the closed-loop system are bounded. Using (17) and Remark 1 yields

$$\begin{aligned} \dot{V} &\le -\kappa_1 s^T s + \|s\|\|\epsilon_1\| \\ &\le -\kappa_1 s^T s + \frac{\|s\|^2}{2} + \frac{\|\epsilon_1\|^2}{2} \\ &\le -(2\kappa_1 - 1)V + \frac{\|\epsilon_1\|^2}{2}. \end{aligned} \tag{18}$$

It follows that

$$V(t) \le V(0)\mathbf{e}^{-(2\kappa_1-1)t} + \frac{||\epsilon_1||^2}{2(2\kappa_1 - 1)} \tag{19}$$

where $\mathbf{e}$ is Euler's number and $V(0) = (1/2)s(0)^T s(0)$.

The above inequality confirms that all the signals s, q and ω are bounded during the transient period of the observer (7).

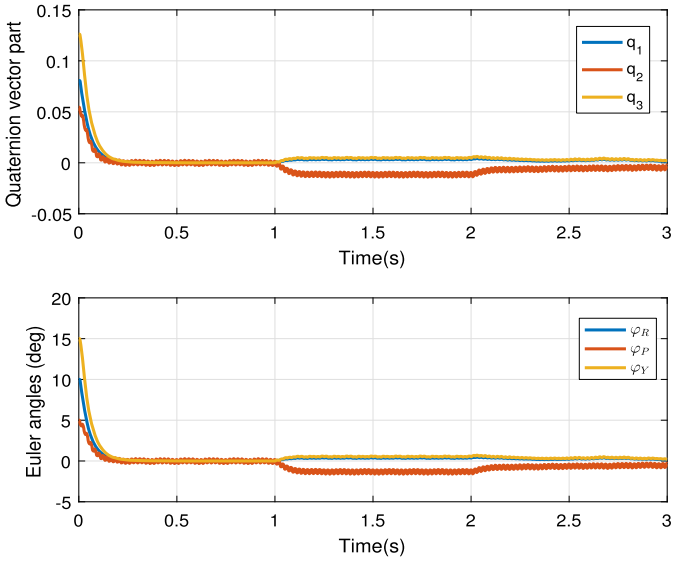

Fig. 3. Attitude response of the conventional SMC method.

Next, we will prove that the sliding motion will occur in finite time. After the finite-time convergence of the observer, e_1 will be zero and (17) reduces to

$$\begin{aligned}\dot{V} &= -\kappa_1 s^T s - \kappa_2 s^T \lfloor s \rceil^{\nu} \\ &= -2\kappa_1 V - \kappa_2 \sum_{i=1}^{3} |s_i|^{1+\nu}. \end{aligned} \tag{20}$$

Applying Lemma 1 to the above equation, it follows that

$$\begin{aligned}\dot{V} &\leq -2\kappa_1 V - \kappa_2 \left(\sum_{i=1}^{3} s_i^2 \right)^{\frac{1+\nu}{2}} \\ &\leq -2\kappa_1 V - 2^{\frac{1+\nu}{2}} \kappa_2 V^{\frac{1+\nu}{2}}. \end{aligned} \tag{21}$$

According to Lemma 2, the sliding motion occurs in finite time, *i.e.*, $s = 0, \forall t \geq t_r$, which implies from Remark 2 that (q, ω) asymptotically goes to the origin along the sliding surface. This completes the proof of Theorem 1. □

Remark 3. If the upper bound of the disturbances $d(t)$ is known in advance, a conventional sliding mode control law could be developed based on [34] for the system (6) with the sliding surface (12) expressed by

$$u = -B^{-1} \left[\left(A\omega + \frac{1}{2} \Gamma T(Q)\omega \right) + \hat{d} + \kappa_1 s + \kappa_2^{SMC} \frac{s}{||s|| + \zeta} \right] \tag{22}$$

where κ_2^{SMC} is bigger than $||d(t)||$ and ζ is a small positive constant to avoid the well-known chattering phenomenon (see [35]).

5. Numerical simulation and discussion

A numerical simulation example is provided to demonstrate the feasibility and performance of the proposed control method. For comparison purpose, the conventional sliding mode controller mentioned in Remark 3 is also applied to a flapping MAV that has wing kinematics and body parameters taking from Tables 1–3 of the paper [9] except that some others are selected as follows:

$$\Phi = 120^o, \qquad \Psi = 120^o,$$

$$r_{cp}^w = [0, \pm \hat{r}_2 R, 0]^T, \qquad r_{Wb}^b = [0, \pm w/2, l_1/2]^T$$

with $\hat{r}_2, R, w$ and l_1 are taken from Table 2 in [9]. Using these parameters and Table 1–2 of the paper [8], we can calculate the stability and control derivatives, and, in turn, obtain the value of the system matrix A and the control matrix B, given by

$$A = \begin{bmatrix} -15.20 & 0 & -19.31 \\ 0 & -2.61 & 0 \\ -8.13 & 0 & -43.18 \end{bmatrix},$$

$$B = \begin{bmatrix} 4275.35 & 2860.64 & 0 \\ 0 & 0 & 3590.66 \\ 2288.51 & 6397.42 & 0 \end{bmatrix}.$$

In this study, it is assumed that the unknown external disturbance torque τ_d is of the form

$$\tau_d(\mu\text{Nm}) = \begin{cases} [0, 0, 0]^T, & t < 1 \\ [20, -20, 10]^T, & 1 \leq t < 2 \\ 10 \times \begin{bmatrix} 2 + 3\cos(3\pi t) \\ -1 - 0.2\sin(2\pi t) \\ 1 + 0.5\sin(t) \end{bmatrix}, & \text{otherwise.} \end{cases} \tag{23}$$

It means that only the modeling uncertainty that cannot be avoided due to the linearization exists during the period $t < 1$.

The parameters of the observer (7), the sliding surface (12), the proposed control law (13) and the conventional SMC controller (22) are chosen as follows

$$L = [1000, 1000, 1000]^T, \qquad n = 2,$$

$$\lambda_0 = 3, \qquad \lambda_1 = 1.5\sqrt{3}, \qquad \lambda_2 = 1.1,$$

$$\Gamma = \text{diag}(20, 20, 20), \qquad \kappa_1 = 20, \qquad \kappa_2 = 500,$$

$$\nu = 0.8, \qquad \kappa_2^{SMC} = 500, \qquad \zeta = 0.01.$$

In addition, the initial states of the observer and the MAVs are selected as $z_0(0) = [0, 0, 0]^T, z_1(0) = z_0(0), z_2(0) = z_0(0), \varphi(0) = [10^o, 5^o, 15^o]^T$ that is equivalent to the quaternion vector part $q(0) = [0.081, 0.054, 0.126]^T$ and $\omega(0) = [0, 0, 0]^T$.

The simulation results of the closed-loop system responses are plotted in Fig. 3–8. Fig. 3 and Fig. 6 show that both of the controllers could quickly stabilize the attitude of the flapping flight in spite of the non-zero initial states and unavoidable modeling uncertainty when $t < 1$. However, when constant external disturbances $(1 \leq t < 2)$ or time-varying external disturbances $(t \geq 2)$, the responses of the flapping flight resulting from two controllers are significantly different. It is clear that the proposed control strategy is capable of substantially eliminating the effects of the external disturbances and the attitude of the flapping flight is rapidly stabilized. In contrast, the conventional SMC controller results in significant steady-state errors. Therefore, it could be concluded that the robustness of the proposed method seems to be better than that of the conventional SMC controller. Figs. 4 and 7 display the waveform of the stroke angles and rotation angles, while Fig. 5 and Fig. 8 depicts mean stroke-plane angles. It can be observed that wing motions and stroke-plane motion of the proposed method are smoother than those of the conventional SMC method, which emphasizes that the proposed method might be more suitable for implementations in practical applications.

6. Conclusions

This paper has introduced an observer-based sliding mode control strategy for stabilizing the attitude of flapping MAVs in the

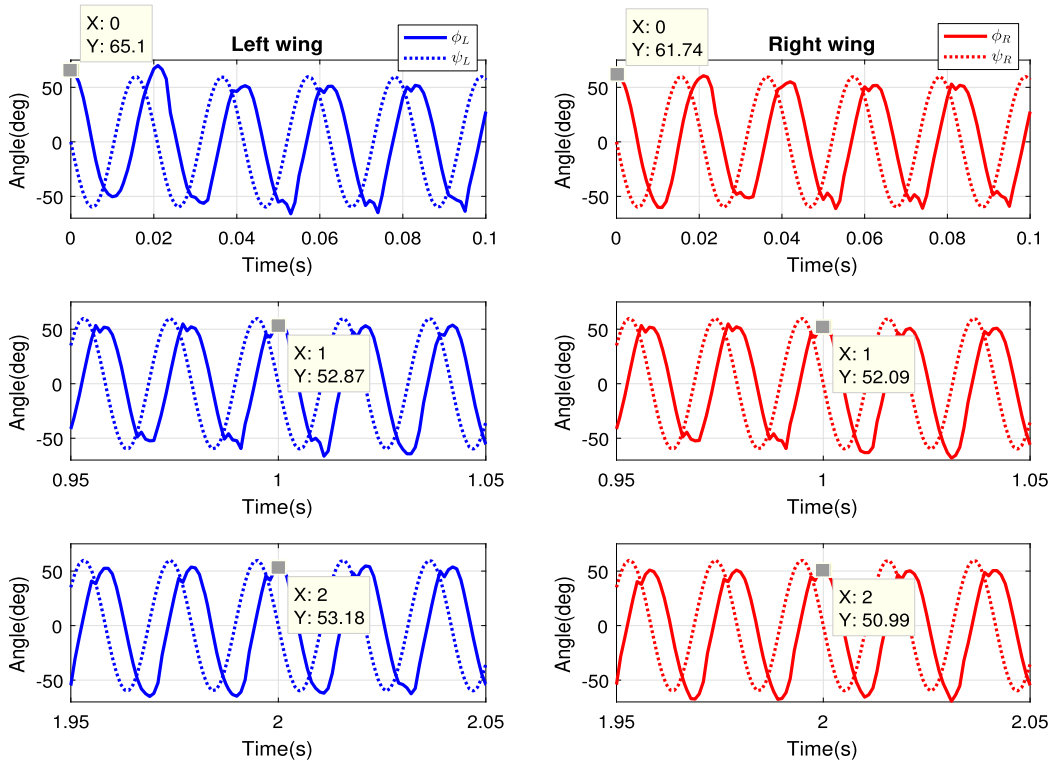

Fig. 4. Time histories of wing kinematics of the conventional SMC method.

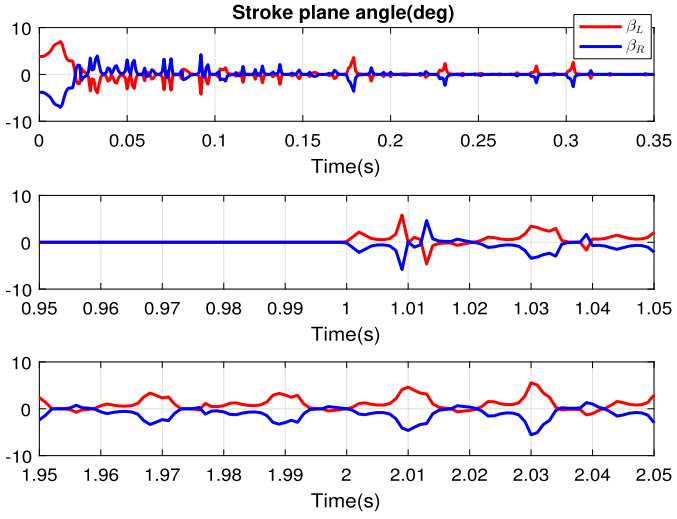

Fig. 5. Time histories of stroke-plane angle of the conventional SMC method.

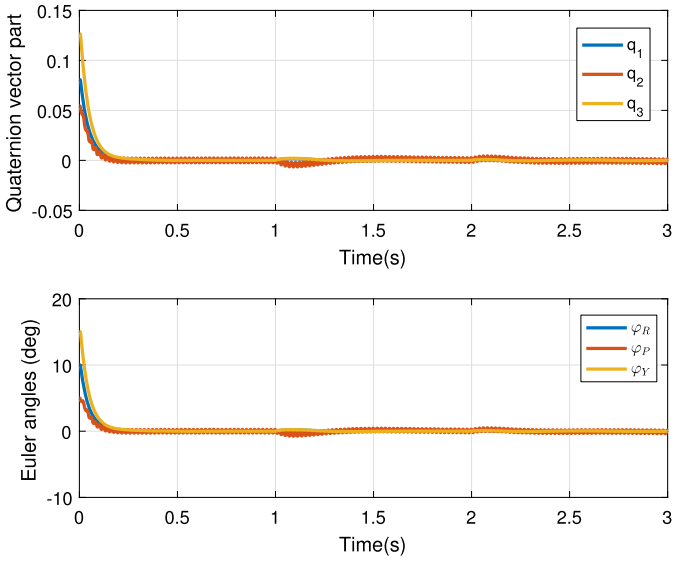

Fig. 6. Attitude response of the proposed control method.

presence of unknown uncertainties and external disturbances. In comparison with the conventional SMC method, the robustness of the proposed method is significantly enhanced because the effect of the lumped disturbances, that is reconstructed by an observer, can be canceled in finite time. A numerical simulation example including the comparison to the conventional SMC method has been carried out to illustrate and evaluate the effectiveness and feasibility of the suggested scheme. It is worth noting that the proposed strategy could be easily extended to the attitude tracking control problem. For future research works, the extension of the paper to the attitude stabilization/attitude tracking control problem of the flapping MAVs without angular velocity measurements should be investigated. Also, the control design can be extended to obtain finite-time attitude stabilization, which consists of promising properties such as robustness, convergence rate, and high accuracy.

Conflict of interest statement

The authors declare that they have no conflict of interest.

Acknowledgements

This research was supported by a grant to Bio-Mimetic Robot Research Center Funded by Defense Acquisition Program Administration and Agency for Defense Development (UD130070ID), Basic Science Research Program through the National Research Foundation of Korea (NRF) funded by the Ministry of Education (2017R1D1A1B03029992) and the 2017 Research Fund

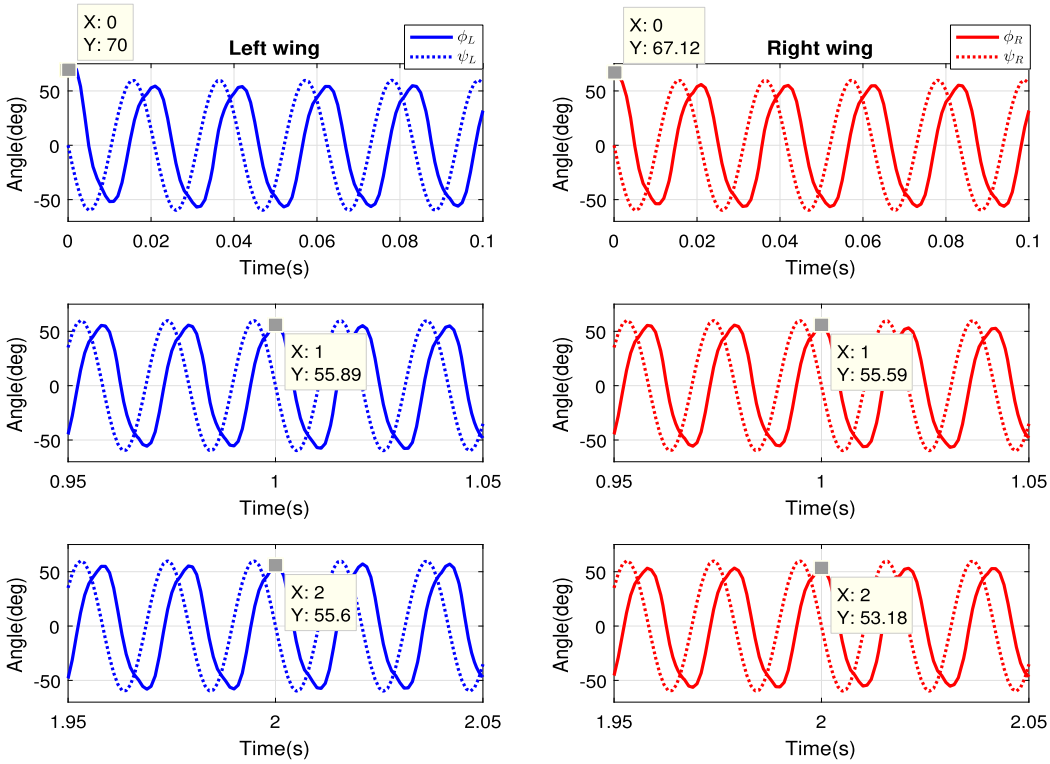

Fig. 7. Time histories of wing kinematics of the proposed control method.

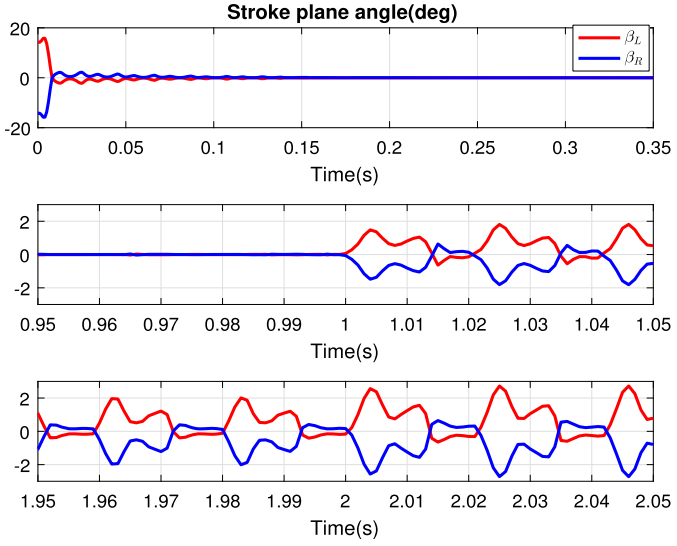

Fig. 8. Time histories of stroke-plane angle of the proposed control method.

(1.170013.01) of UNIST (Ulsan National Institute of Science and Technology).

References

[1] C.T. Orlowski, A.R. Girard, Dynamics, stability, and control analyses of flapping wing micro-air vehicles, Prog. Aerosp. Sci. 51 (2012) 18–30.
[2] M. Sun, Insect flight dynamics: stability and control, Rev. Mod. Phys. 86 (2014) 615–646.
[3] C. Zhang, C. Rossi, A review of compliant transmission mechanisms for bio-inspired flapping-wing micro air vehicles, Bioinspir. Biomim. 12 (2017) 025005.
[4] Y. Nan, M. Karásek, M.E. Lalami, A. Preumont, Experimental optimization of wing shape for a hummingbird-like flapping wing micro air vehicle, Bioinspir. Biomim. 12 (2017) 26010.
[5] S.F. Armanini, M. Karásek, G.C.H.E. de Croon, C.C. de Visser, Onboard/offboard sensor fusion for high-fidelity flapping-wing robot flight data, J. Guid. Control Dyn. 40 (2017) 2121–2132.
[6] C. Badrya, A. Sridharan, J.D. Baeder, C.M. Kroninger, Multi-fidelity coupled trim analysis of a flapping-wing micro air vehicle flight, J. Aircr. 54 (2017) 1614–1630.
[7] C.T. Orlowski, A.R. Girard, W. Shyy, Open Loop Pitch Control of a FlappingWing Micro AirVehicle Using a Tail and Control Mass, 2010, pp. 536–541.
[8] B. Cheng, X. Deng, Near-hover dynamics and attitude stabilization of an insect model, in: Proc. 2010 Am. Control Conf, 2010, pp. 39–44.
[9] M. Karasek, A. Preumont, Simulation of flight control of a hummingbird like robot near hover, Acta Tech. 58 (2013) 119–139.
[10] X. Deng, L. Schenato, S.S. Sastry, Flapping flight for biomimetic robotic insects: part II-flight control design, IEEE Trans. Robot. 22 (2006) 776–788.
[11] M. Sun, J.K. Wang, Flight stabilization control of a hovering model insect, J. Exp. Biol. 210 (2007) 2714–2722.
[12] J.E. Bluman, C.-K. Kang, Y.B. Shtessel, Sliding mode control of a biomimetic flapping wing micro air vehicle in hover, AIAA Atmos. Flight Mech. Conf. (2017) 1–16.
[13] P. Chirarattananon, K.Y. Ma, R.J. Wood, Adaptive control of a millimeter-scale flapping-wing robot, Bioinspir. Biomim. 9 (2014) 25004.
[14] P. Chirarattananon, Y. Chen, E.F. Helbling, K.Y. Ma, R. Cheng, R.J. Wood, Dynamics and flight control of a flapping-wing robotic insect in the presence of wind gusts, Interface Focus 7 (2017) 20160080.
[15] V.I. Utkin, Sliding Modes in Control Optimization, first ed., Springer, Berlin, Heidelberg, 1992.
[16] J.Y. Hung, W. Gao, J.C. Hung, Variable structure control: a survey, IEEE Trans. Ind. Electron. 40 (1993) 2–22.
[17] F. Plestan, Y. Shtessel, V. Bregeault, A. Poznyak, New methodologies for adaptive sliding mode control, Int. J. Control 83 (2010) 1907–1919.
[18] J. Yang, S. Li, X. Yu, Sliding-mode control for systems with mismatched uncertainties via a disturbance observer, IEEE Trans. Ind. Electron. 60 (2013) 160–169.
[19] S. Li, J. Yang, W.H. Chen, X. Chen, Disturbance Observer-based Control: Methods and Applications, Taylor & Francis, Boca Raton, 2014.
[20] W.H. Chen, J. Yang, L. Guo, S. Li, Disturbance-observer-based control and related methods – an overview, IEEE Trans. Ind. Electron. 63 (2016) 1083–1095.
[21] P. Freymuth, Thrust generation by an airfoil in hover modes, Exp. Fluids 9 (1990) 17–24.
[22] W. Shyy, Y. Lian, J. Tang, D. Viieru, H. Liu, Aerodynamics of Low Reynolds Number Flyers, Cambridge University Press, New York, 2007.
[23] S.P. Sane, M.H. Dickinson, The aerodynamic effects of wing rotation and a revised quasi-steady model of flapping flight, J. Exp. Biol. 205 (2002) 1087–1096.

[24] X. Deng, L. Schenato, S.S. Sastry, Flapping flight for biomimetic robotic insects: part I-system modeling, IEEE Trans. Robot. 22 (2006) 776–788.
[25] G.K. Taylor, A.L.R. Thomas, Dynamic flight stability in the desert locust Schistocerca gregaria, J. Exp. Biol. 206 (2003) 2803–2829.
[26] J.R. Wertz, Spacecraft Attitude Determination and Control, Kluwer Academic, Dordrecht, 1990, pp. 410–435.
[27] B. Cheng, X. Deng, Translational and rotational damping of flapping flight and its dynamics and stability at hovering, IEEE Trans. Robot. 27 (2011) 849–864.
[28] C. Edwards, S. Spurgeon, Sliding Mode Control: Theory and Applications, Taylor & Francis, London, 1998, pp. 31–33.
[29] Y.B. Shtessel, I.A. Shkolnikov, A. Levant, Smooth second-order sliding modes: missile guidance application, Automatica 43 (2007) 1470–1476.
[30] A. Levant, M. Livne, Exact differentiation of signals with unbounded higher derivatives, IEEE Trans. Autom. Control 57 (2012) 1076–1080.
[31] E. Bechkenback, R. Bell Man, Inequalities, Springer-Verlag, Berlin, 1961, pp. 18–19.
[32] S. Yu, X. Yu, B. Shirinzadeh, Z. Man, Continuous finite-time control for robotic manipulators with terminal sliding mode, Automatica 41 (2005) 1957–1964.
[33] S.-C. Lo, Y.-P. Chen, Smooth sliding-mode control for spacecraft attitude tracking maneuvers, J. Guid. Control Dyn. 18 (1995) 1345–1349.
[34] X.-Y. Lu, S.K. Spurgeon, Robust sliding mode control of uncertain nonlinear systems, Syst. Control Lett. 32 (1997) 75–90.
[35] J.A. Burton, A.S.I. Zinober, Continuous approximation of variable structure control, Int. J. Syst. Sci. 17 (1986) 875–885.